TRANSPORT PHENOMENA IN ZONAL CENTRIFUGE ROTORS

I. Velocity and Shear-Stress Distributions of Fluid during Acceleration

H. W. HSU

From The Molecular Anatomy Program, Oak Ridge National Laboratory, Oak Ridge, Tennessee 37830. Dr. Hsu's present address is the Department of Chemical and Metallurgical Engineering, The University of Tennessee, Knoxville, Tennessee 37916.

ABSTRACT An analysis is presented for the evaluation of velocity components and shear-stress distributions of fluid in zonal centrifuge rotors during acceleration. Analytical expressions for the distribution of tangential and radial velocity components and the tangential shear-stress and the radial shear-stress distributions of fluid are obtained for the transient case. Characteristics of each distribution for a typical density gradient liquid in a zonal centrifuge rotor are computed from the relations derived, and are presented as figures. An unusual phenomenon—the tangential velocity of the gradient exceeding the velocity of the rotor during a particular period of acceleration—is demonstrated.

INTRODUCTION

Zonal centrifuges have been developed for the mass separation of subcellular particles and viruses on the basis of either sedimentation rate or buoyant density (1–8). They have been made with various numbers of septa and have been used to isolate major subcellular components, viruses (4, 5, 9, 10), ribosomal RNA (11), and serum macroglobulins. For a micromolecular separation, very high speed rotors are favored; for obtaining a high resolution and for large-particle separation, low speed rotors are required. From a mechanical design point of view, a rotor without septa is preferred for high speed operations. For large-particle separation, movement of whole cells into septa may occur. Therefore, it would be of interest to separate large particles in a reorienting gradient rotor without septa. Thus, both very low and very high speed rotors may require use of reorienting gradient rotors. Previous studies and current literature on the rotors do not provide us with information needed to predict optimal configurations and conditions of rotor operations. Here, a simple zonal centrifuge rotor without septa was studied. In the subsequent studies, the effect of different numbers of septa and internal rotor configuration on resolution, especially after reorientation, etc. will be investigated. The objective of the present study was the quantitative evaluation of velocity components and shear-stress distributions of fluid in zonal centrifuge rotor operations. An adequate knowledge of various velocity components of fluid in zonal centrifuge rotors will permit the rational selection of centrifuge conditions for mass separation of new biomaterials. Knowledge of shear-stress distributions of fluid in the rotors will guide the control of rotor acceleration to prevent damage to biomaterials being separated.

FORMULATION OF PROBLEM

We consider a cylinder of radius R filled with a fluid whose density increases linearly with distance r from the axis. The cylinder is to rotate about its own axis at an angular velocity Ω. When the cylinder is rotating at a steady state, the fluid in the cylinder moves as the elements of rigid body (12). Thus, the tangential velocity component, V_θ, is ΩR, the radial velocity component, V_r, is zero, and there is no shear stress existing within the fluid. Shear stress will arise only during the acceleration or deceleration periods. The equations of motion governing the transient behavior of the fluid in a cylindrical container (centrifuge rotor) rotating about its own axis can be formulated as follows, using cylindrical coordinates for convenience. As the rotor's angular velocity increases from Ω_i to Ω_f, the radial and axial velocity components of fluid, V_r and V_z will be smaller by orders of magnitude than the tangential velocity component, V_θ of fluid. Thus, the motion of fluid can be adequately represented by the tangential component velocity alone. This is given by (reference 12):

$$\frac{\partial V_\theta}{\partial t} = \nu_0(1 + \epsilon r) \frac{\partial}{\partial r}\left[\frac{1}{r}\frac{\partial}{\partial r}(rV_\theta)\right]. \tag{1}$$

The initial and boundary conditions for the case are:

$$V_\theta(0, r) = 0 \tag{2a}$$

$$V_\theta(t, R) = \Delta\Omega R(1 - e^{-at}) \tag{2b}$$

$$V_\theta(t, 0) = 0 \tag{2c}$$

where $\Delta\Omega$ is the change of rotor's angular velocity expressed by the quantity $(\Omega_f - \Omega_i)$ and a is the time constant in an equation describing the control of the rotor's acceleration or deceleration.

SOLUTION OF EQUATION

Equations 1 and 2 can be rewritten with reduced independent variables. These are

$$\frac{\partial V_\theta}{\partial \tau} = \frac{1}{\zeta}\frac{\partial V_\theta}{\partial \zeta} - \frac{V_\theta}{\zeta^2} + \frac{\partial^2 V_\theta}{\partial \zeta^2} + \lambda\left[\frac{\partial V_\theta}{\partial \zeta} - \frac{V_\theta}{\zeta} + \zeta\frac{\partial^2 V_\theta}{\partial \zeta^2}\right] \tag{3}$$

$$V_\theta(0, \zeta) = 0 \tag{4a}$$

$$V_\theta(\tau, 1) = \Delta\Omega R[1 - e^{-(\alpha/\nu_0)\tau}] \tag{4b}$$

$$V_\theta(\tau, 0) = 0 \tag{4c}$$

where

$$\tau = \frac{\nu_0 t}{R^2}, \quad \zeta = \frac{r}{R}, \quad \epsilon R = \lambda, \quad \text{and} \quad \alpha = aR^2. \tag{5a, b, c, d}$$

Equation 3 is to be solved by the method of separation of variables. If it is assumed that

$$V_\theta = T(\tau)Z(\zeta), \tag{6}$$

one will obtain the following two ordinary differential equations from equation 3:

$$\frac{dT}{d\tau} = -b^2 T \tag{7}$$

$$(1 + \lambda\zeta)\frac{d^2Z}{d\zeta^2} + \frac{(1 + \lambda\zeta)}{\zeta}\frac{dZ}{d\zeta} - \left(\frac{1 + \lambda\zeta - b^2\zeta}{\zeta^2}\right)Z = 0 \tag{8}$$

in which b^2 is a constant or constants (eigenvalues). Equation 7 can be easily integrated to give the solution

$$T = Be^{-b^2\tau}. \tag{9}$$

The quantity B is a constant. Equation 8 is solved by the method of Frobenius (13). If one assumes that the solution can be expressed as a power series,

$$Z = \sum_{j=0}^{\infty} A_j \zeta^{m+j} \tag{10}$$

then, substituting equation 10 into equation 8, one obtains the following conditions in order to satisfy the equation

$$A_0(m^2 - 1) = 0 \tag{11a}$$

$$A_1[(m + 1)^2 - 1] + A_0\lambda(m^2 - 1) = 0 \tag{11b}$$

$$A_{j+2}[(m + j + 2)^2 - 1] + A_{j+1}\lambda[(m + j + 1)^2 - 1] - A_j b^2 = 0 \tag{11c}$$

Inspection of equation 11a shows that the indicial equation is

$$m = \pm 1, \tag{12}$$

then, from equations 11*b* and 12, one obtains

$$A_1 = 0. \tag{13}$$

With $m = 1$ and equation 11*c* as a recurrence equation, the coefficients, A_j, in equation 10 can be expressed in terms of A_0. These are

$$A_2 = \frac{b^2}{3^2 - 1} A_0 \tag{14a}$$

$$A_3 = \frac{-b^2\lambda}{4^2 - 1} A_0 \tag{14b}$$

$$A_4 = \frac{b^2}{5^2 - 1}\left(\frac{b^2}{3^2 - 1} + \lambda^2\right) A_0 \tag{14c}$$

$$A_5 = \frac{-b^2}{6^2 - 1}\left(\frac{b^2}{4^2 - 1} + \frac{b^2}{3^2 - 1} + \lambda^2\right) A_0 \tag{14d}$$

$$A_6 = \frac{b^2}{7^2 - 1}\left[\frac{b^2}{5^2 - 1}\left(\frac{b^2}{3^2 - 1} + \lambda^2\right) + \left(\frac{b^2}{4^2 - 1} + \frac{b^2}{3^2 - 1} + \lambda^2\right)\lambda^2\right] A_0 \tag{14e}$$

$$A_7 = \frac{-b^2\lambda}{8^2 - 1}\left[\frac{b^2}{6^2 - 1}\left(\frac{b^2}{4^2 - 1} + \frac{b^2}{3^2 - 1} + \lambda^2\right) + \frac{b^2}{5^2 - 1}\left(\frac{b^2}{3^2 - 1} + \lambda^2\right) + \left(\frac{b^2}{4^2 - 1} + \frac{b^2}{3^2 - 1} + \lambda^2\right)\lambda^2\right] A_0 \tag{14f}$$

$$A_8 = \frac{b^2}{9^2 - 1}\left(\left\{\frac{b^2}{7^2 - 1}\left[\frac{b^2}{5^2 - 1}\left(\frac{b^2}{3^2 - 1} + \lambda^2\right) + \left(\frac{b^2}{4^2 - 1} + \frac{b^2}{3^2 - 1} + \lambda^2\right)\lambda^2\right] + \left[\frac{b^2}{6^2 - 1}\left(\frac{b^2}{4^2 - 1} + \frac{b^2}{3^2 - 1} + \lambda^2\right) + \frac{b^2}{5^2 - 1}\left(\frac{b^2}{3^2 - 1} + \lambda^2\right) + \left(\frac{b^2}{4^2 - 1} + \frac{b^2}{3^2 - 1} + \lambda^2\right)\lambda^2\right]\lambda^2\right\}\right) A_0. \tag{14h}$$

$\vdots$ $\vdots$

With $m = -1$ and equation 11*c* as a recurrence equation, one obtains the coefficients, A_j as follows:

$$A_0 = A_1 = 0; \qquad A_2 \neq 0 \text{ (the lowest coefficient)} \tag{15}$$

$$A_3 = 0 \tag{15a}$$

$$A_4 = \frac{b^2}{3^2 - 1} A_2 \tag{15b}$$

$$A_5 = -\frac{b^2\lambda}{4^2 - 1} A_2 \tag{15c}$$

$$A_6 = \frac{b^2}{5^2 - 1}\left(\frac{b^2}{3^2 - 1} + \lambda^2\right) A_2 \tag{15d}$$

$$\vdots \qquad\qquad \vdots$$

By inspecting equation 11*b*, one also has the following results in order to satisfy equation 10:

$$A_0 = 0 \tag{16}$$

$$A_1 \neq 0; \qquad A_1[(m + 1)^2 - 1] = 0. \tag{16a}$$

Then, the indicial equation is

$$m = 0 \quad \text{or} \quad -2. \tag{17}$$

If $m = 0$, using equation 11*c* as a recurrence equation, one gets

$$A_2 = 0 \tag{18a}$$

$$A_3 = \frac{b^2}{3^2 - 1} A_1 \tag{18b}$$

$$A_4 = \frac{-b^2\lambda}{4^2 - 1} A_1 \tag{18c}$$

$$A_5 = \frac{b^2}{5^2 - 1}\left(\frac{b^2}{3^2 - 1} + \lambda^2\right) A_1 \tag{18d}$$

$$\vdots \qquad\qquad \vdots$$

If $m = -2$, with equation 11*c* as a recurrence equation, one has

$$A_0 = A_1 = A_2 = 0; \qquad A_3 \neq 0 \tag{19}$$

$$A_4 = 0 \tag{19a}$$

$$A_5 = \frac{b^2}{3^2 - 1} A_3 \tag{19b}$$

$$A_6 = \frac{-b^2\lambda}{4^2 - 1} A_3 \tag{19c}$$

$$A_7 = \frac{b^2}{5^2 - 1}\left(\frac{b^2}{3^2 - 1} + \lambda^2\right) A_3 \tag{19d}$$

$$\vdots \qquad\qquad \vdots$$

It might seem, therefore, that we have obtained four independent solutions, which is, of course, impossible. Closer inspection shows that all four solutions are identical, so $A_0 = A_2 = A_1 = A_3$ for all four solutions. Thus, the solution for $Z = f(\zeta)$ is:

$$Z_1 = A\cdot\zeta \left[\begin{array}{l} 1 + \frac{b^2}{3^2 - 1}\zeta^2 - \frac{b^2\lambda}{4^2 - 1}\zeta^3 + \frac{b^2}{5^2 - 1}\left(\frac{b^3}{3^2 - 1} + \lambda^2\right)\zeta^4 \\ - \frac{b^2\lambda}{6^2 - 1}\left(\frac{b^2}{4^2 - 1} + \frac{b^2}{3^2 - 1} + \lambda^2\right)\zeta^5 \\ + \frac{b^2}{7^2 - 1}\left[\frac{b^2}{5^2 - 1}\left(\frac{b^2}{3^2 - 1} + \lambda^2\right) + \left(\frac{b^2}{4^2 - 1} + \frac{b^2}{3^2 - 1}\right.\right. \\ \left.\left. + \lambda^2\right)\lambda^2\right]\zeta^6 - \frac{b^2}{8^2 - 1}\left[\frac{b^2}{6^2 - 1}\left(\frac{b^2}{4^2 - 1} + \frac{b^2}{3^2 - 1} + \lambda^2\right)\right. \\ \left. + \frac{b^2}{5^2 - 1}\left(\frac{b^2}{3^2 - 1} + \lambda^2\right) + \left(\frac{b^2}{4^2 - 1} + \frac{b^2}{3^2 - 1} + \lambda^2\right)\lambda^2\right]\zeta^7 \\ + \frac{b^2}{9^2 - 1}\left\{\frac{b^2}{7^2 - 1}\left[\frac{b^2}{5^2 - 1}\left(\frac{b^2}{3^2 - 1} + \lambda^2\right) + \left(\frac{b^2}{4^2 - 1} + \frac{b^2}{3^2 - 1}\right.\right.\right. \\ \left.\left. + \lambda^2\right)\lambda^2\right] + \left[\frac{b^2}{6^2 - 1}\left(\frac{b^2}{4^2 - 1} + \frac{b^2}{3^2 - 1} + \lambda^2\right)\right. \\ \left.\left. + \frac{b^2}{5^2 - 1}\left(\frac{b^2}{3^2 - 1} + \lambda^2\right) + \left(\frac{b^2}{4^2 - 1} + \frac{b^2}{3^2 - 1} + \lambda^2\right)\lambda^2\right]\lambda^2\right\}\zeta^8 \\ - \cdots \end{array}\right] \tag{20}$$

or

$$Z = A\left(\zeta - \frac{b^2}{3^2 - 1}\zeta^3 + \frac{b^2\lambda}{4 - 1}\zeta^4\right) + \sum_{j=0}^{\infty} A_{j+5}\,\zeta^{j+5} \tag{20a}$$

in which

$$A_{j+5} = \frac{A_{j+3}\,b^2 - A_{j+4}\,\lambda[(j + 4)^2 - 1]}{(j + 5)^2 - 1}. \tag{20b}$$

The series representation of Z becomes divergent after the fourth term. Thus, in order to have a finite value of Z, the series has to be terminated after some finite number of terms. At some finite j, there must exist the eigenvalues

$$b_j^2 = \frac{A_{j+4}}{A_{j+3}}\lambda[(j + 4)^2 - 1] \tag{21}$$

such that the series will have a finite value. From equation 21 the first few eigenvalues are evaluated and are as follows:

$$b_0^2 = -8.0000\,\lambda^2$$

$$b_1^2 = -5.2174\,\lambda^2$$
$$b_2^2 = -4.2857\,\lambda^2$$
$$b_3^2 = -3.8182\,\lambda^2$$
$$b_4^2 = -3.5368\,\lambda^2$$
$$b_5^2 = -3.3488\,\lambda^2$$
$$b_6^2 = -3.2143\,\lambda^2$$
$$\vdots \qquad \vdots \tag{22}$$

With these eigenvalues, the Z-equation, after simplification, becomes:

$$Z = A\cdot\zeta\begin{bmatrix}1 - \lambda^2\zeta^2 + 0.5333\,\lambda^3\zeta^3 - 0.1160\,\lambda^4\zeta^4 + 0.0142\,\lambda^5\zeta^5 \\ -0.0011\,\lambda^6\zeta^6 + 0.00006\,\lambda^7\zeta^7 - 0.00003\,\lambda^8\zeta^8 + \cdots\end{bmatrix} \tag{23}$$

Then, with equation 9, the tangential component velocity, V_θ, becomes:

$$V_\theta = A\cdot\zeta\begin{bmatrix}e^{-b_0^2\tau} - (\lambda^2\zeta^2 - 0.5333\,\lambda^3\zeta^3)e^{-b_1^2\tau} - 0.1160\,\lambda^4\zeta^4 e^{-b_2^2\tau} \\ + 0.0142\,\lambda^5\zeta^5 e^{-b_3^2\tau} - 0.0011\,\lambda^6\zeta^6 e^{-b_4^2\tau} + 0.00006\,\lambda^7\zeta^7 e^{-b_5^2\tau} \\ - 0.00003\,\lambda^8\zeta^8 e^{-b_6^2\tau} + \cdots\end{bmatrix}. \tag{24}$$

The constant A in equation 24 is determined from the boundary condition, equation 4b. The tangential component velocity, V_θ, becomes:

$$V_\theta = \Delta\Omega R(1 - e^{-(\alpha/\nu_0)\tau})\cdot\zeta$$
$$\begin{bmatrix}1 - (1 - 0.5333\,\lambda\zeta)\cdot\lambda^2\zeta^2 e^{-2.7826\lambda^2\tau} - 0.1160\,\lambda^3\zeta^3 e^{-3.7143\lambda^2\tau} \\ + 0.0142\,\lambda^5\zeta^5 e^{-4.1818\lambda^2\tau} - 0.0011\,\lambda^6\zeta^6 e^{-4.4632\lambda^2\tau} \\ + 0.00006\,\lambda^7\zeta^7 e^{-4.6512\lambda^2\tau} - 0.00003\,\lambda^8\zeta^8 e^{-4.7857\lambda^2\tau} \\ - \cdots\end{bmatrix}$$
$$\begin{bmatrix}1 - (1 - 0.5333\lambda)\lambda^2 e^{-2.7826\lambda^2\tau} - 0.1160\,\lambda^4 e^{-3.7143\lambda^2\tau} \\ + 0.0142\,\lambda^5 e^{-4.1818\lambda^2\tau} - 0.0011\,\lambda^6 e^{-4.4632\lambda^2\tau} \\ + 0.00006\,\lambda^7 e^{-4.6512\lambda^2\tau} - 0.00003\,\lambda^8 e^{-4.7857\lambda^2\tau}\end{bmatrix}^{-1}. \tag{25}$$

The radial component velocity, V_r, is related to the tangential component velocity, V_θ, by the sedimentation coefficient, s, in such a manner that

$$s = \frac{dr/dt}{\Omega^2 r} = \frac{V_r}{V_\theta^2/r} \tag{26a}$$

$$V_r = \frac{V_\theta^2}{r}\cdot s. \tag{26b}$$

Therefore, an expression for the radial component velocity is obtained.

SHEAR-STRESS DISTRIBUTIONS

The shear-stress distributions, $\tau_{r\theta}(\zeta)$ and $\tau_{rr}(\zeta)$, the tangential shear-stress, and the radial shear-stress distributions, now may be obtained from the velocity distributions. The tangential shear-stress distribution, $\tau_{r\theta}(\zeta)$ is given as (reference 12);

$$\tau_{r\theta} = \tau_{\theta r} = -\mu\left[r\frac{\partial}{\partial r}\left(\frac{V_\theta}{r}\right)\right] = -\frac{\mu_0}{R}(1+\delta\zeta)\cdot\zeta\frac{\partial}{\partial\zeta}\left(\frac{V_\theta}{\zeta}\right). \quad (27)$$

After differentiation, the reduced tangential shear-stress distribution may be expressed as follows:

$$\frac{\tau_{r\theta}}{\Delta\Omega\mu_0} = (1+\delta\zeta)(1-e^{-(\alpha/\nu_0)\tau})$$

$$\begin{bmatrix} (2\lambda^2\zeta^2 - 1.5999\,\lambda^3\zeta^3)e^{-2.7826\lambda^2\tau} + 0.4640\,\lambda^4\zeta^4e^{-3.7143\lambda^2\tau} \\ -\,0.0710\,\lambda^5\zeta^5e^{-4.1818\lambda^2\tau} + 0.0066\,\lambda^6\zeta^6e^{-4.4632\lambda^2\tau} \\ -\,0.00042\,\lambda^7\zeta^7e^{-4.6512\lambda^2\tau} + 0.00024\,\lambda^8\zeta^8e^{-4.7857\lambda^2\tau} \\ -\cdots \end{bmatrix}$$

$$\begin{bmatrix} 1-(1-0.5333\,\lambda)\lambda^2e^{-2.7828\lambda^2\tau} - 0.1160\,\lambda^4e^{-3.7143\lambda^2\tau} \\ +\,0.0142\,\lambda^5e^{-4.1818\lambda^2\tau} - 0.0011\,\lambda^6e^{-4.4632\lambda^2\tau} \\ +\,0.00006\,\lambda^7e^{-4.6512\lambda^2\tau} - 0.00003\,\lambda^8e^{-4.7857\lambda^2\tau} \\ +\cdots \end{bmatrix}^{-1}. \quad (28)$$

In a similar manner, the radial shear-stress distribution, $\tau_{rr}(\zeta)$ may be obtained. It

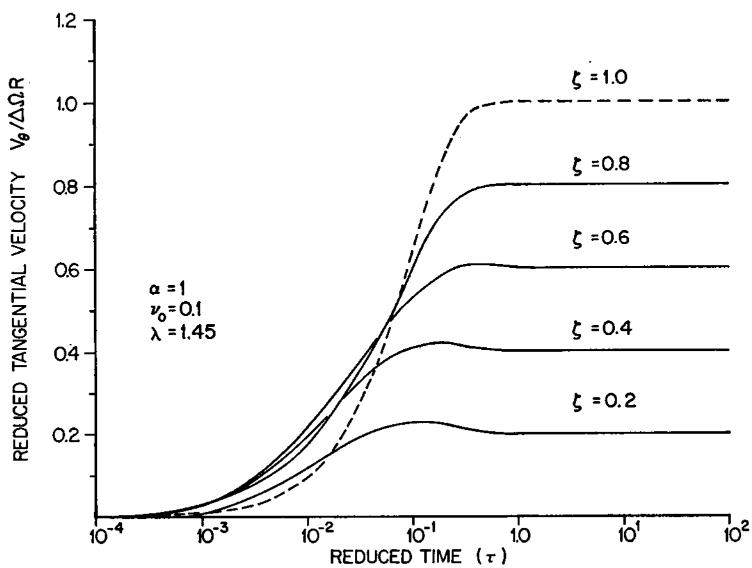

FIGURE 1 Tangential component velocity distributions in the rotor with $\alpha = 1$, $\nu_0 = 0.1$, and $\lambda = 1.45$.

is given by (reference 12):

$$\begin{aligned}\tau_{rr} &= -\mu\left(2\frac{\partial V_r}{\partial r}\right)\\ &= -\frac{\mu_0}{R}(1+\delta\zeta)\cdot 2\frac{\partial V_r}{\partial\zeta}\\ &= -\mu\left[2\frac{\partial}{\partial r}\left(\frac{sV_\theta^2}{r}\right)\right]\\ &= -\frac{2\,s\mu_0(1+\delta\zeta)}{R^2}\frac{\partial}{\delta\zeta}(V_\theta^2/\zeta).\end{aligned} \tag{29}$$

Finally, the reduced radial shear-stress distribution is:

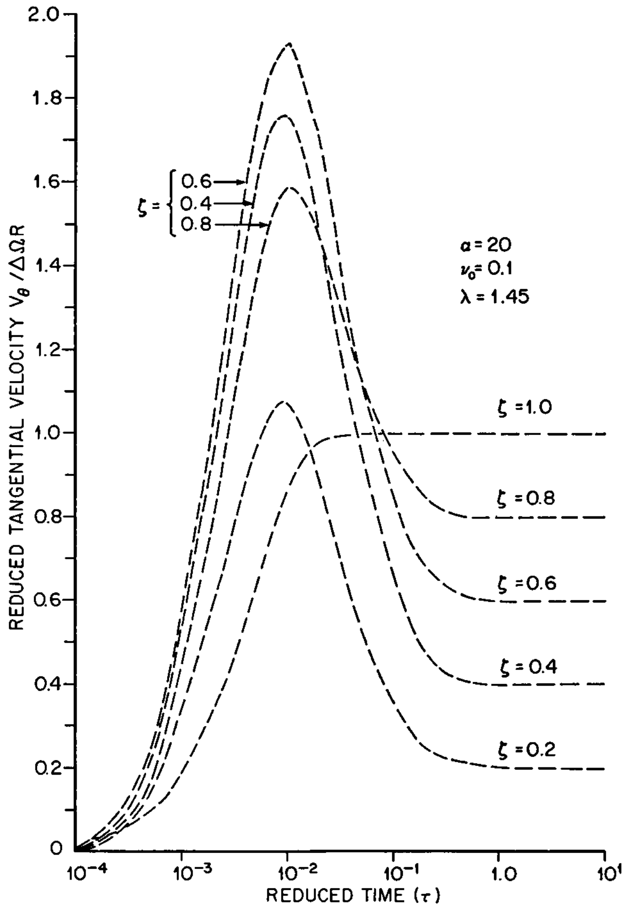

FIGURE 2 Tangential component velocity distributions in the rotor with $\alpha = 20$, $\nu_0 = 0.1$, and $\lambda = 1.45$.

$$\frac{\tau_{r\tau}}{2\Delta\Omega^2\mu_0 s} = (1 + \delta\zeta)(1 - e^{-(\alpha/\nu_0)\lambda})^2$$

$$\begin{bmatrix} 1 - (3 - 2.1332\,\lambda\zeta)\,\lambda^2\zeta^2 e^{-2.7826\lambda^2\tau} - 0.5800\,\lambda^4\zeta^4 e^{-3.7143\lambda^2\tau} \\ + 0.0852\,\lambda^5\zeta^5 e^{-4.1818\lambda^2\tau} - 0.0077\,\lambda^6\zeta^6 e^{-4.4632\lambda^2\tau} \\ + 0.00048\,\lambda^7\zeta^7 e^{-4.6512\lambda^2\tau} - 0.00027\,\lambda^8\zeta^8 e^{-4.7857\lambda^2\tau} \\ + \cdots \end{bmatrix}$$

$$\begin{bmatrix} 1 - (1 - 0.5333\,\lambda\zeta)\,\lambda^2\zeta^2 e^{-2.7826\lambda^2\tau} - 0.1160\,\lambda^4\zeta^4 e^{-3.7143\lambda^2\tau} \\ + 0.0142\,\lambda^5\zeta^5 e^{-4.1818\lambda^2\tau} - 0.0011\,\lambda^6\zeta^6 e^{-4.4632\lambda^2\tau} \\ + 0.0006\,\lambda^7\zeta^7 e^{-4.6512\lambda^2\tau} - 0.00003\,\lambda^8\zeta^8 e^{-4.7857\lambda^2\tau} \\ + \cdots \end{bmatrix}$$

$$\begin{bmatrix} 1 - (1 - 0.5333\,\lambda)\lambda^2 e^{-2.7826\lambda^2\tau} - 0.1160\,\lambda^4 e^{-3.7143\lambda^2\tau} \\ + 0.0142\,\lambda^5 e^{-4.1818\lambda^2\tau} - 0.0011\,\lambda^6 e^{-4.4632\lambda^2\tau} \\ + 0.0006\,\lambda^7 e^{-4.6512\lambda^2\tau} - 0.00003\lambda^8 e^{-4.7857\lambda^2\tau} \\ + \cdots \end{bmatrix}^{-2}. \tag{30}$$

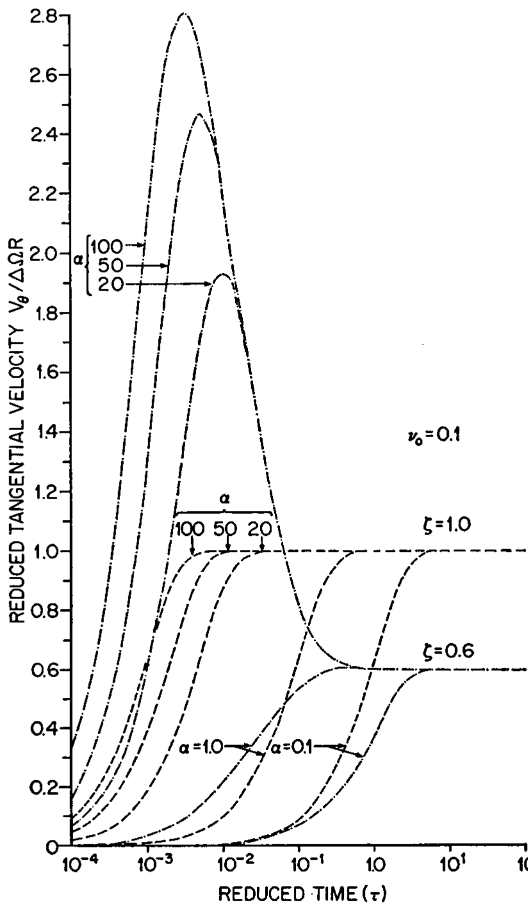

FIGURE 3 Variation of tangential component velocity distributions with time constants.

The biomaterials, or the macromolecules, are suspended in the gradient solution. Under the centrifugal force field, the motion of those macromolecules may be reasonably approximated by the motion of the part of the gradient through which they are sedimenting. Therefore, the shear stresses the macromolecules will receive during the rotation of the rotor are similar to those experienced by the part of the gradient solution through which they are sedimenting. Hence, we can treat the shear-stress distributions of fluid as the shear stresses macromolecules will experience during the rotation of zonal rotors.

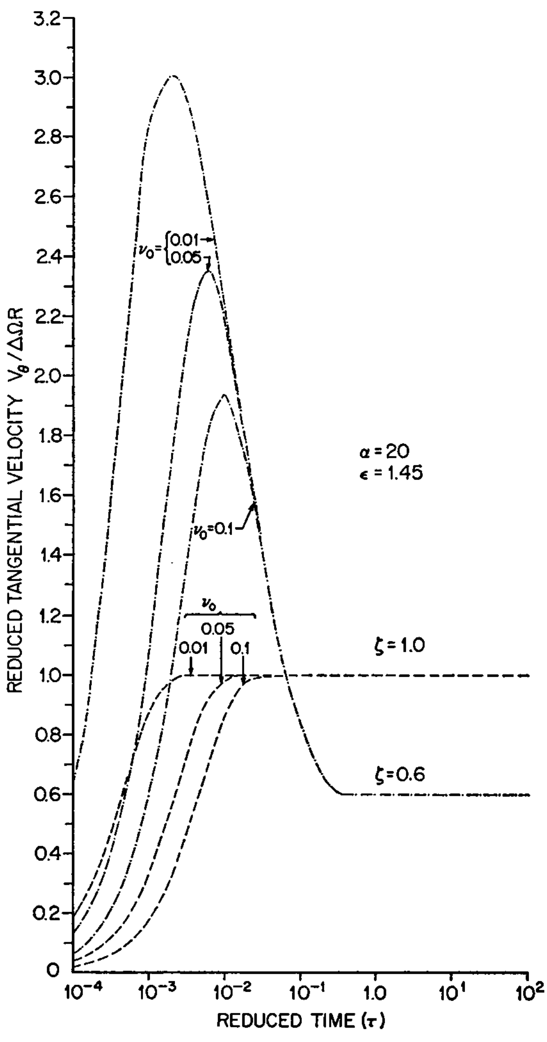

FIGURE 4 Variation of tangential component velocity distributions with the reference kinematic viscosity at the axis of the rotor.

PROPERTIES OF SOLUTIONS

A FORTRAN program for an IBM 360 series digital computer was written to calculate velocities and shear stresses from equations 25, 28, and 3 to permit evaluation of the characteristics of the mathematical results obtained. The parametric values, $\lambda = 1.45$ and $\delta = 1.66$ were used in the calculations, since these values apply to a sucrose gradient solution with concentration varying from 10 to 30% across the rotor. The results were plotted in graphical forms as a function of reduced time.

Figs. 1 and 2 present the reduced local tangential velocity distributions in the rotor as a function of reduced time with the reference kinematic viscosity at the axis of

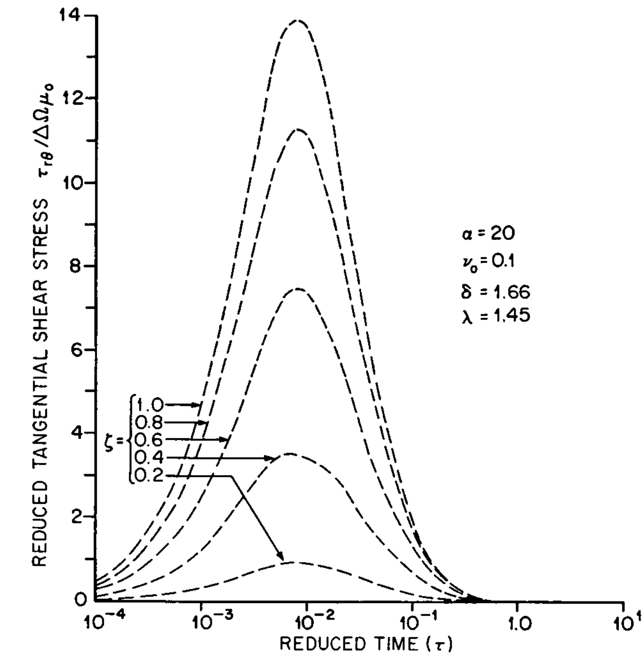

FIGURE 5 Tangential shear-stress distributions in the rotor with $\alpha = 20$, $\nu_0 = 0.1$, $\lambda = 1.45$, and $\delta = 1.66$.

the rotor, $\nu_0 = 0.1$, and the reduced time constant expressing the control of the rotor's acceleration, $\alpha = 1$ and 20, respectively. Fig. 3 shows the reduced tangential velocities of the rotor at the wall and of the gradient at 60% of the radial distance from the axis to the wall as functions of reduced time with $\nu_0 = 0.1$ and values of the reduced time constant varying from 0.1 to 100. These results demonstrate the effect of the reduced time constant on the tangential velocity distributions. Fig. 4 illustrates the effect of variation of the kinematic viscosity on the tangential velocity distributions for ν_0 varying from 0.01 to 0.1.

A rather unusual phenomenon was observed in these results. The local tangential velocity of the gradient solution exceeds the velocity of the rotor during a particular period of acceleration. The degree of excess for the velocity in the gradient increases with increasing time constant and decreases with increasing kinematic viscosity. This phenomenon may be explained as follows: the rate of acceleration of the rotor is governed by the rate controlling expression, equation 2*b*. The rate of acceleration increases rather slowly during the starting period, gradually increases to a maximum,

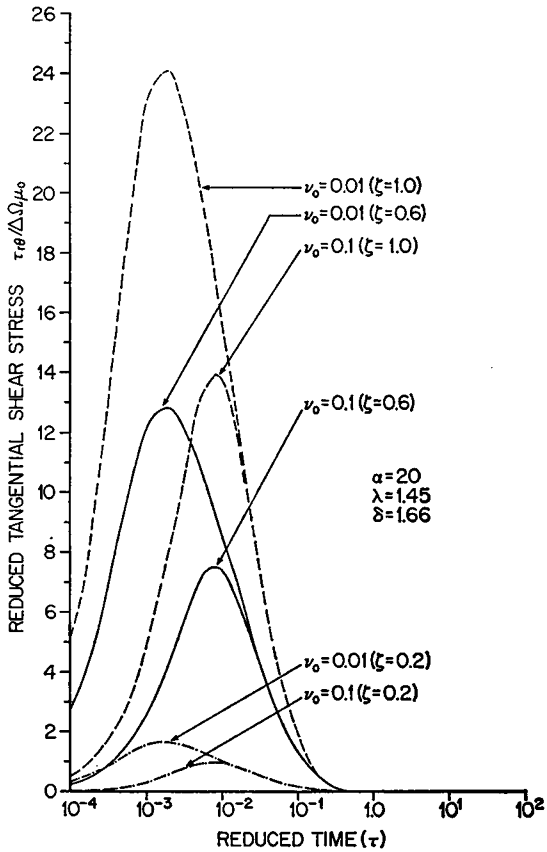

FIGURE 6 Variation of tangential shear-stress distributions with the reference kinematic viscosity at the axis of the rotor.

then diminishes, and finally approaches zero at a steady state. The motion in the gradient is induced by the momentum transfer from the rotor wall to the axis through the gradient. While the rotor is accelerated by the controlling expression, the gradient is accelerated by the energy transferred from the rotor wall. In the gradient, the viscosity decreases linearly with distance from the wall toward the axis. When the rotor reaches its maximum acceleration, its energy transfers to a position of the gradient where the friction due to the local viscosity is much less than the frictional loss resulting from the momentum transfer to that location, and a much greater rate of acceleration is induced in the gradient. Thus, the velocity at that location exceeds the velocity of the rotor. When the gradient acquires this maximum momentum due to the maximum rate of acceleration of the rotor and induces the maximum velocity, the rotor itself is already accelerating at a much slower rate. Thus, following the rate-controlling expression of the rotor, the maximum velocity in the gradient diminishes quickly and approaches its stable, steady-state velocity $\Omega\zeta$.

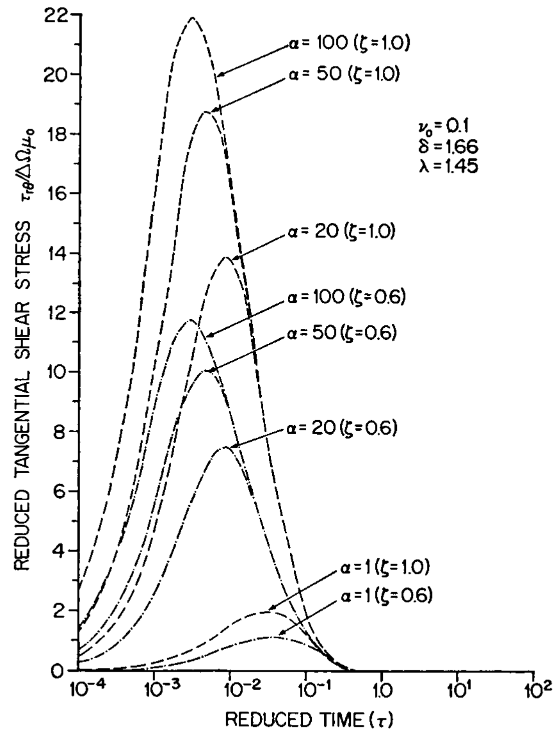

FIGURE 7 Variation of tangential shear-stress distributions with time constants.

The tangential shear-stress distributions are presented in Figs. 5–7. Fig. 5 shows the tangential shear-stress distributions in the gradient for the case where $\alpha = 20$ and $\nu_0 = 0.1$. Fig. 6 demonstrates the effect of ν_0 on the tangential shear-stress distributions when $\alpha = 20$. Fig. 7 illustrates the effect of α on the tangential shear-stress distributions for $\nu_0 = 0.1$. The tangential shear stress increases with increasing α and decreases with increasing ν_0.

Figs. 8 and 9 show the variation of radial shear-stress distributions with time. For the case where $\alpha = 20$ and $\nu_0 = 0.1$, the radial shear-stress distributions in the gradient are shown in Fig. 8. Fig. 9 demonstrates the effects of α and ν_0 on the radial

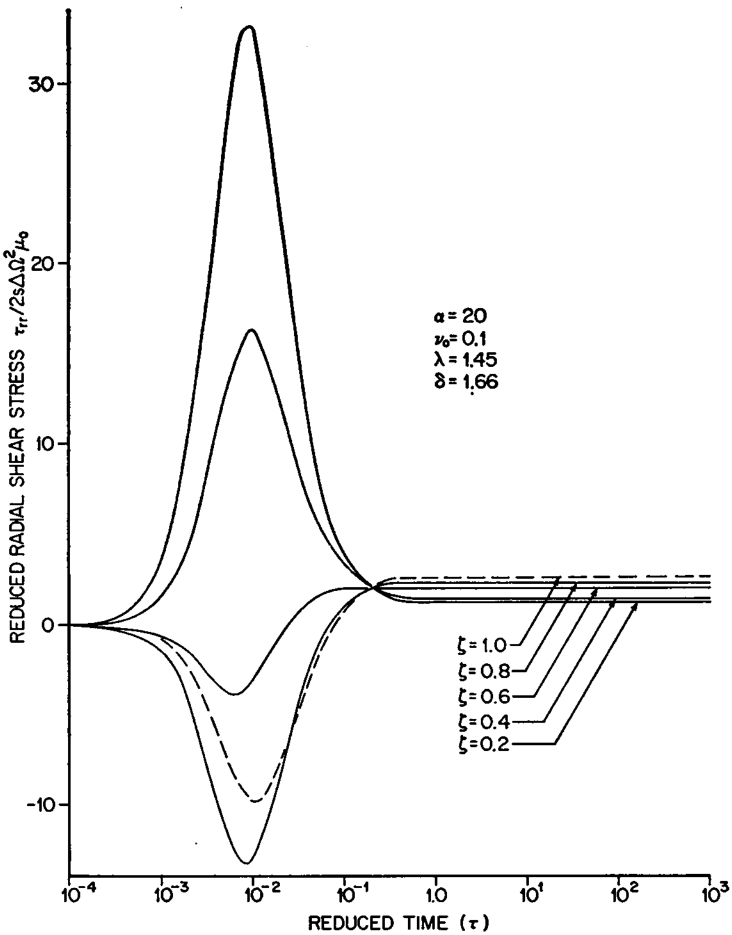

FIGURE 8 Radial shear-stress distributions in the rotor with $\alpha = 20$, $\nu_0 = 0.1$, $\lambda = 1.45$, and $\delta = 1.66$.

shear-stress distributions. During a certain period of acceleration, radial shear stress within the gradient reverses direction. This suggests a turbulence or mixing motion during acceleration period which disappears as a steady state is approached.

DISCUSSION

These results are based on three approximations: (*a*) that the rotor (cylinder) is so long that there is no end effect in the axial direction, (*b*) that the radial and the axial velocity components are so small compared with the tangential velocity component that they are negligible during the acceleration, and (*c*) that the sedimentation coefficient is a constant. These approximations are considered reasonable, therefore permitting with relative ease the development of analytical solution. Without these

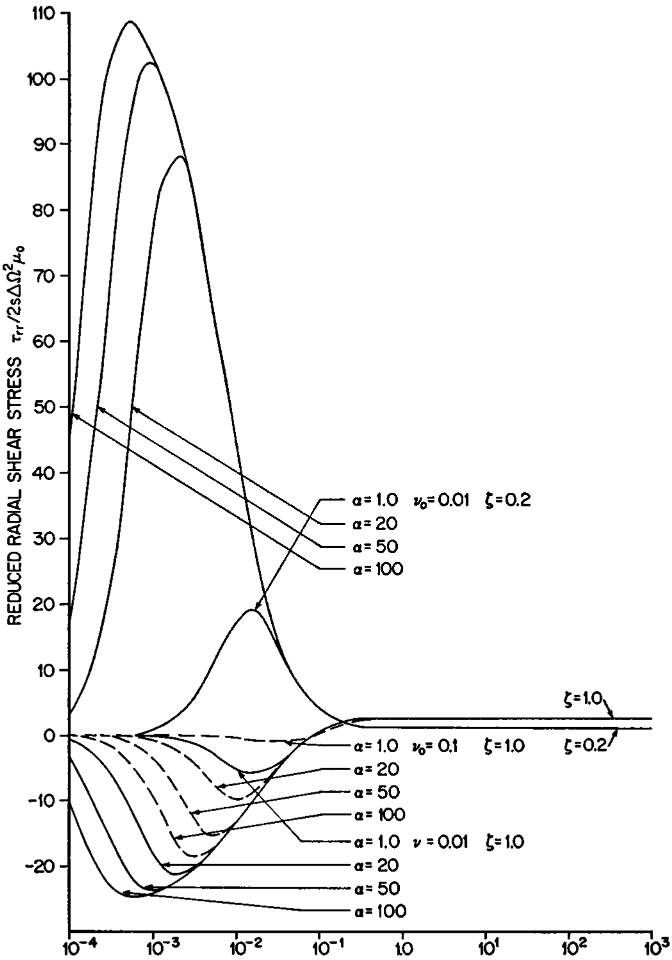

FIGURE 9 Variation of radial shear-stress distributions with time constants and the reference kinematic viscosity at the axis of the rotor.

simplifications, one must solve simultaneously the three-coupled time-dependent Navier-Stokes equations in cylindrical coordinates by numerical methods of questionable accuracy and stability.

The estimates provided by the analysis of velocity components and shear-stress distributions during acceleration serve as a guide for controlling the acceleration of the rotor to its maximum speed to prevent damage to biomaterial being separated. They also can guide control of the deceleration of the rotor to a full stop, particularly for a reorienting gradient rotor, to assure that the separated biomaterial does not remix during the deceleration period.

An excess tangential velocity component of the gradient in the rotor with the dyed beads of various densities suspended in the gradient solution during the acceleration period can be observed with the naked eye. We are in the process of recording this phenomenon by using an accurate instrumentation technique. In the subsequent investigations, the effect of different numbers of septa and internal rotor configurations on resolution and isodensity reorienting gradient rotors, etc. will be considered.

NOMENCLATURE

a	time constant
A	constant
A_j	coefficients of power series
b^2	characteristic constant(s) (eigenvalues)
B	constant
m	characteristic values in the indicial equation
r	radius variable
R	radius of rotor
s	sedimentation coefficient
t	time variable
T	function of time variable
V_r	radial component velocity
V_θ	tangential component velocity
Z	function of radius variable
α	constant defined in equation *5d*
ρ	density
μ	dynamic viscosity
ν	kinematic viscosity $\nu = \mu/\rho$
τ	reduced time $\tau = \nu_0 t/R^2$
ζ	reduced radius $\zeta = r/R$
Ω	angular velocity
τ_{ij}	shear-stress tensor
ϵ	characteristic constant for kinematic viscosity variation
λ	characteristic constant for kinematic viscosity variation in rotor, $\lambda = \epsilon R$
δ	characteristic constant for dynamic viscosity variation in rotor
Subscripts	
0	quantity evaluated at reference condition
1, 2, 3,...	indices of the coefficient
r	radius direction
θ	angular direction
j	summation index

The author wishes to express his sincere appreciation to Dr. Norman G. Anderson and Mr. C. T. Rankin, Jr. for their valuable discussions and constant encouragement and also to acknowledge with thanks the assistance of Mr. R. A. Carter, who computed the numerical results.
Research was supported by the NIH-AEC Molecular Anatomy Program jointly sponsored by the National Cancer Institute, the National Institute of Allergy and Infectious Disease, the National Institute of General Medical Science, and the U.S. Atomic Energy Commission.

H. W. Hsu is with the Biology Division, Oak Ridge National Laboratory, as a consultant. Research at the Oak Ridge National Laboratory is sponsored by the U.S. Atomic Energy Commission under contract with Union Carbide Corporation.

Received for publication 22 December 1967 and in revised form 3 June 1968.

REFERENCES

1. Anderson, N. G. 1962. *J. Phys. Chem.* **66**:1984.
2. Anderson, N. G., and C. L. Burger. 1963. *Science.* **136**:646.
3. Anderson, N. G. 1963. *Federation Proc.* **22**:674.
4. Anderson, N. G. 1963. *Nature.* **199**:1166.
5. Anderson, N. G., C. L. Burger, and W. W. Harris. 1963. *J. Cell Biol.* **19**:12A.
6. Anderson, N. G., H. P. Barringer, E. F. Babelay, and W. D. Fisher. 1964. *Life Sci.* **3**:667.
7. Anderson, N. G. 1966. *In* The Development of Zonal Centrifuges and Ancillary Systems for Tissue Fractionation and Analysis. N. G. Anderson, editor. Natl. Cancer Inst. Monograph. **21**:9. U.S. Government Printing Office, Washington, D.C.
8. Barringer, H. P., N. G. Anderson, C. E. Nunley, K. T. Ziehlke, and W. S. Dritt. 1966. *In* The Development of Zonal Centrifuges and Ancillary Systems for Tissue Fractionation and Analysis. N. G. Anderson, editor. Natl. Cancer Inst. Monograph. **21**:165. U.S. Government Printing Office, Washington, D.C.
9. Reimer, C. B., T. E. Newlin, M. L. Havens, R. S. Baker, N. G. Anderson, G. B. Cline, H. P. Barringer, and C. E. Nunley. 1966. *In* The Development of Zonal Centrifuges and Ancillary Systems for Tissue Fractionation and Analysis. N. G. Anderson, editor. Natl. Cancer Inst. Monograph. **21**:375. U.S. Government Printing Office, Washington, D.C.
10. Reimer, C. B., Robert S. Baker, Thomas E. Newlin, Milton L. Havens. 1966. *Science.* **152**: 1379.
11. Hastings, J. R. B., J. H. Parish, K. S. Kirby, and E. S. Klucis. 1965. *Nature.* **208**:646.
12. Bird, R. B., W. E. Stewart, and E. N. Lightfoot. 1960. Transport Phenomena. McGraw-Hill Book Co., New York.
13. Margenau, H., and G. M. Murphy. 1955. The Mathematics of Physics and Chemistry. Van Nostrand Book Co., Princeton, N. J.